Classical dynamics study of atomic oxygen sticking on the β-cristobalite (100) surface

C. Arasa [a], H. F. Busnengo [b], A. Salin [c] and R. Sayós [a]

[a] *Departament de Química Física and Institut de Química Teòrica i Computacional, Universitat de Barcelona, C. Martí i Franquès 1, 08028 Barcelona, Spain*
[b] *Instituto de Física Rosario, CONICET and Facultad de Ciencias Exactas, Ingeniería y Agrimensura, Univ. Nacional de Rosario, Av. Pellegrini 250, 2000 Rosario, Argentina*
[c] *Lab. Physico-Chimie Moléculaire, UMR 5803 CNRS-Univ. Bordeaux I, 351 Cours de la Libération, 33405 Talence Cedex, France*

Abstract

The sticking of oxygen atoms with collision energies in the range 0.1-1 eV on a clean (100) β-cristobalite surface with surface temperatures between 300-1100 K has been investigated using classical trajectories for normal and off-normal incidence. A full dimensional adiabatic potential energy surface (PES) based on a dense grid of density functional theory (DFT) points was constructed by means of the corrugation reducing procedure. Sticking probabilities are very high (> 0.9) for all conditions, increasing with collision energy and decreasing with surface temperature. This behavior can be interpreted by decomposing the sticking between adsorption and absorption, which show different trends. The large attractive character of the PES favors the absorption or penetration into the big unit cell of the β-cristobalite, with a predominant direct mechanism instead of a dynamic trapping, accordingly also with the quick dissipation of the oxygen energy into the slab. Calculated thermal initial sticking coefficients seem to depend on the type of silica structure. Moreover, these initial thermal coefficients are much higher than values derived using expressions obtained from standard transition state theory even when using as parameters values extracted from DFT calculations. Therefore, the use of these expressions in kinetic models for O or N recombination over silica should be reconsidered

Keywords: Adsorption, sticking, absorption, reflection, diffusion, cristobalite, silica, atomic oxygen, classical trajectories, dynamics, density functional theory.

Figures: 8

Proofs to: Dr. R. Sayós

***** Corresponding author: e-mail: r.sayos@ub.edu

1. Introduction

The atomic and molecular oxygen interaction on silica-based materials has a lot of interest because of its importance in the heterogeneous chemical processes that take place over the thermal protection system (TPS) of some spacecrafts (e.g., Space Shuttle) during their terrestrial re-entry [1]. Silicon dioxide is an important material used in coating materials for some parts of these vehicles. For instance, reaction-cured glass (RCG) with 94% of SiO_2, 4% of B_2O_3 and 2% of SiB_4 is normally used in Space Shuttle tiles.

The main processes involving the TPS materials and the dissociated air (e.g., in Earth's atmosphere) produced by the shockwave are the TPS oxidation, with the formation of an oxide layer, and several heterogeneous catalytic atomic recombinations. The exothermic heterogeneous processes can increase the total heat transfer to the vehicle at the hypersonic flight velocities. Catalytic heating accounts for 25-35% of the total heating at surface temperatures near the critical temperature during re-entry. TPSs composed by materials as little catalytic as possible are searched to reduce the vehicle heating. For this purpose, several SiO_2-based materials are used although the slight catalysis of these materials should be taken into account more accurately to improve the quality of the kinetic models, which assume an ideal non-catalytic surface approximation. The mechanisms and the rates of the different gas-surface processes in such non-equilibrium conditions (i.e., hypersonic flows) are not well known [2]. In fact, much of these processes have neither been well characterized even at room temperature. For this reason, accurate theoretical and experimental data are necessary to simulate (e.g., via computational fluid dynamics (CFD) codes) hypersonic spacecrafts flights with several TPS materials.

In spite of the major abundance of N_2 compared to O_2 in air, the much lower O_2 dissociation energy favors the atomic oxygen abundance and hence that the subsequent O recombinations through the Eley-Rideal (ER) or Langmuir-Hinshelwood (LH) mechanisms become more important in these conditions. The first common step to either ER or LH processes is the atomic oxygen adsorption. Nevertheless, scarce experimental data are available about atomic or molecular oxygen adsorption over silica surfaces. Furthermore, most of the experimental kinetic models for air recombination over several types of silica materials (i.e., Pyrex, quartz, RCG, etc.) assume an average value of 3.5 eV [1] for the adsorption energy of either O or N, although some values within the range of 2.6-5.5 eV [3-7] have also been used. These adsorption energies are indirectly derived from kinetic models that fit experimental ER/LH data. Thus, for instance, initial sticking coefficients S_0 of $0.05e^{-0.002T}$ (on SiO_2) or $1.0e^{-0.002T}$ (on

RCG) and an oxygen adsorption energy of 3.5 eV have been reported for both surfaces [1] following these procedures. There are also recent experimental measurements [8-9] about the oxygen recombination coefficient (γ_O) over silica indicating that this coefficient is a factor of three-times lower in β-quartz than in β-cristobalite, showing thus the importance of the silica structure in these processes.

In a previous work [10], we presented a wide density functional theory study (DFT) on the lowest triplet (quartet) and singlet (doublet) stationary points of the lowest potential energy surfaces (PES) corresponding to O and N interaction, respectively, with β-cristobalite (100)-Si or O face ended; β-cristobalite is a polymorph of silica [11-12], stable at high temperatures up to the melting point of 1983 K, although is also metaestable at room temperature. This crystalline solid has similar properties to amorphous silica, like density, refractive index, band structure, etc, and seems to be a good candidate for modeling the amorphous silica coatings used in TPSs. Our DFT study showed that O and N become strongly adsorbed over the first silicon face of β-cristobalite, mainly on top Si and over a bridge between two Si atoms. The calculated average adsorption energies of O were equal to 5.89 eV (for the singlet state) and 4.87 eV (for the triplet state), much higher than the supposed value of 3.5 eV used in before mentioned kinetic models.

In the present work, we examine the interaction of O atoms with a β-cristobalite (100) surface in order to get information about the sticking and reflection probabilities and to clarify the microscopic mechanism of this interaction. We will present the construction of an interpolated PES founded on new and extensive DFT data, which will be used to run classical trajectories under several initial conditions of surface temperature (T_S), O kinetic energy (E_i) and incident angle (θ_i). The results will be compared with a previous dynamics study based on a less accurate PES [13] on this system along with the available theoretical or experimental data on these or related processes.

2. DFT calculations on the ground PES

We have carried out DFT calculations by means of the VASP code [14-17] to determine the atomic oxygen interaction with a Fdd2 β-cristobalite (100) surface [18-19] for a grid of oxygen positions (X_O,Y_O, Z_O) over the square 1x1 unit cell (Fig. 1(a)), using a SiO_2 slab model including 6 layers with a silicon first layer. A lattice parameter of 7.348 Å, determined for the bulk Fdd2 structure, was used in the present calculations. Details of this kind of calculations

were reported in a previous study [10]. The slab geometry was kept fixed at its most stable configuration in absence of O atom. An additional hydrogen bottom layer was added to saturate the O dangling bonds of the inner layer. The distance between slabs (ca. z = 17-18 Å) was large enough to prevent significant interactions between them. DFT calculations were based on the generalized gradient correction functional Perdew-Wang 91 (PW91). The electron-ion interactions were described by using the projector-augmented-wave technique. For the plane wave basis set, an energy cut-off of 400 eV was accurate enough to obtain converged properties. Integration over the Brillouin zone was made by means of a 3x3x1 k-points mesh by using the Monkhorst-Pack method.

Spin-polarized calculations with a fixed magnetization equal to 0 and 2 were carried out to consider the total spin states (i.e., singlet and triplet) derived from atomic oxygen in the ground state (triplet) and β-cristobalite (singlet). Moreover, calculations with free magnetization were almost coincident with the lowest spin state energies. In general, when the distance between the impinging oxygen atom and its nearest neighbor substrate atoms is greater than 2.5 Å, the lowest energy corresponds to the triplet state but when the O atom approaches the surface, the singlet state has a lower energy than the triplet one.

Throughout this paper, we assume that the evolution of the system is electronically adiabatic (i.e., the force acting on the impinging O atom arises from the locally lowest PES) which entails at least one transition between states of different spin. The general validity of this assumption in gas-surface interactions has been challenged for the case of O_2/Al(111) [20]. However, a rigorous formalism allowing to go beyond the adiabatic approximation for gas-surface systems is not yet well established. Thus, the analysis of the electronically adiabatic dynamics, which has been widely used to investigate atomic chemisorption (e.g., O/Cu(100), [21], N/W(100) [22], N/SiO_2 [23],..), can be an excellent starting point for the study of O adsorption on SiO_2 from first principles electronic structure calculations. On the other hand, the existence of abundant experimental data for O recombination reaction over several silica surfaces (e.g., RCG, pyrex, quartz, cristobalite,..) and the usual guess of the previous O chemisorption over the Si atoms, introduced commonly in all kinetic models [1], can support more the use of the adiabatic approximation.

Besides the previous O adsorption minimum on top Si (T1, [10]), the use of the new interpolated PES (see next section) has allowed the finding of another adsorption minimum (T1'), slightly more stable than the T1 or B1 adsorption minima. This new minimum corresponds to a O-Si bond with an angle respect the normal to the surface (θ) of 77.1° (in T1

was θ = 0°) and along the positive slope diagonal (T1-B1-T1) of the unit cell (Fig. 1(a)), but with a O-Si distance (R_{OSi} = 1.559 Å) similar to that of T1 minimum. Both Si atoms become much closer (R_{SiSi} = 3.444 Å) than in the clean slab (R_{SiSi} = 5.196 Å) but only a SiO bond is formed, contrary to what happens for B1 minimum [10], also located over this diagonal. The T1' minimum has an adsorption energy of 6.55 eV compared with the value of 6.05 eV found for T1. The harmonic vibrational frequencies (870.6, 235.7, 185.2 cm^{-1}) confirm that it is a true minimum. There is a small barrier of 0.16 eV between T1 and T1', which corresponds to a transition state at R_{OSi} = 1.519 Å, θ = 10.5° and R_{SiSi} = 4.963 Å, with harmonic vibrational frequencies of 207.5i, 207.2, 157.7 cm^{-1}. This small energy barrier will be negligible for the dynamics of O gas collisions over β-cristobalite.

3. Interpolated PES: construction and analysis

The PES for an atom-solid surface system (i.e., oxygen-β-cristobalite) can be expressed as a sum of two potentials:

$$V^{PES}(X_O, Y_O, Z_O, \{R_{ij}\}) = V^{slab}(\{R_{ij}\}) + V^{O-slab}(X_O, Y_O, Z_O, \{R_{ij}\}) \qquad (1)$$

which depends on the oxygen Cartesian coordinates over the unit cell and on all internuclear distances $\{R_{ij}\}$ (i.e., O-O, Si-O and Si-Si) inside the silica slab. The first term on the r.h.s. of (1) describes the interaction between atoms inside the slab in the absence of the O adsorbate. We describe it by means of a sum of pair interactions inside the silica:

$$V^{slab}(\{R_{ij}\}) = \sum_{i=1}^{N_O}\sum_{i<j}^{N_O} \phi_{OO}(R_{ij}) + \sum_{i=1}^{N_{Si}}\sum_{i<j}^{N_{Si}} \phi_{SiSi}(R_{ij}) + \sum_{i=1}^{N_{Si}}\sum_{j=1}^{N_O} \phi_{SiO}(R_{ij}) \qquad (2)$$

where N_O and N_{Si} are the total number of O and Si atoms of the slab, respectively. For each pair interaction we have used an empirical potential based on a modified form of the Born-Mayer-Huggins ionic potential:

$$\phi_{ij}(R_{ij}) = A_{ij} e^{-R_{ij}/\rho} + \frac{Z_i Z_j}{R_{ij}} \mathrm{erfc}\left(\frac{R_{ij}}{\beta_{ij}}\right) \quad (in\ au) \qquad (3)$$

where R_{ij} is the interatomic distance between i and j atom, Z_i is the formal ionic charge, and A_{ij}, β_{ij} and ρ are empirical parameters. These potentials have been successfully employed in earlier molecular dynamics of silica and silicate systems [24-25] and also in our previous PES (called hereafter as PES-2B) for this system [13]. The bulk Si-O pair-wise interactions are attractive whereas the O-O and Si-Si interactions are repulsive. The empirical potential defined by (2) and (3) reproduces quite well the bulk geometry of β-cristobalite: R_{SiO} = 1.602-1.656 Å, average angle <SiOSi = 170.1º and average angle <OSiO = 106.5º. These values would correspond to a DFT structure intermediate between Fd3m and Fdd2 space group symmetries, which present similar cohesive energies and very small differences in their geometries [10]. Thus the average SiOSi angle is in between 180º (Fd3m) and 147.5 º (Fdd2) DFT values; the average OSiO angle is still much closer to the bulk DFT values of β-cristobalite [10].

The second term on the r.h.s. of (1) contains the interaction between the incident oxygen atom and the β-cristobalite (100) surface. It has been approximated as:

$$V^{O-slab}(X_O, Y_O, Z_O, \{R_{ij}\}) = V_{eq}^{O-slab}(X_O, Y_O, Z_O, \{R_{ij}\}_{eq}) + \left[\sum_{i=1}^{N_{Si}} V_{OSi}(R_{O\,i}) - V_{OSi}(R_{O\,i\,eq})\right] + \left[\sum_{j=1}^{N_O} V_{OO}(R_{O\,j}) - V_{OO}(R_{O\,j\,eq})\right] \quad (4)$$

It means that we assume that the change in the PES due to slab atom displacements can be accounted for by means of O-O and O-Si pairwise interactions. Thus, both sums in (4) will give the energy change for O/slab interaction when moving atoms i (Si) or j (O) from its equilibrium slab position. This approximation was previously used too and justified for a CRP PES of the O/Cu(100) system [21].

The construction of this $V^{O\text{-}slab}$ potential is based on a grid of DFT points calculated over a reduced cell (the triangle in Fig. 1(a)) with a mesh of 0.4 Å in X_O and Y_O and a mesh of 0.25 Å in Z_O, within the interval -1 Å ≤ Z_O ≤ 3 Å (3400 points). Energies are generated over the complete 1x1 square unit cell using its symmetry. Interpolation between calculated DFT points is achieved through the corrugation-reducing procedure (CRP) interpolation method [26], widely applied in several atom or diatomic molecule/metal surface systems [21-22, 27-29]. Its key feature consists in reducing the variation of DFT potential energy by substraction of O-O and O-Si pair interactions:

$$I^{3D}(X_O, Y_O, Z_O, \{R_{ij}\}_{eq}) = V_{DFT}^{O-slab}(X_O, Y_O, Z_O, \{R_{ij}\}_{eq}) - \sum_{j=1}^{N_O'} V_{OSi}(R_{O\,j\,eq}) - \sum_{i=1}^{N_{Si}'} V_{OO}(R_{O\,i\,eq}) \quad (5)$$

The V_{OSi} and V_{OO} potentials were derived by using the DFT energies corresponding to the interaction of O over T1 (i.e., a Si atom of the first layer) and S2 (i.e., an O atom of the second layer) sites as a function of Z_O. Thus, I^{3D} becomes exactly zero for these points. These pair potentials go to zero when $R_{O\,k} = Z_O \geq 3$ Å (hence that $N_{O'} < N_O$ and $N_{Si'} < N_{Si}$).

Interpolation in Z over the calculated values is achieved by an 1D cubic spline. We have verified that the variation of I^{3D} with X_O, Y_O and Z_O is much smoother, which has two consequences. On the one hand, interpolation of I^{3D} over X_O, Y_O and Z_O can be achieved accurately by a 3D cubic spline, which would not have been the case if the DFT values had been interpolated directly. On the other hand, the latter observation proves that the stronger contribution to the forces arises from the latter two terms on the r.h.s. of (5). Accordingly, this justifies the use of the same potentials for V_{OSi} and V_{OO} in (4), which yields the final expression:

$$V^{O-slab}(X_O, Y_O, Z_O, \{R_{ij}\}) = I^{3D}(X_O, Y_O, Z_O, \{R_{ij}\}_{eq}) + \sum_{i=1}^{N_{Si}'} V_{OSi}(R_{O\,i}) + \sum_{j=1}^{N_O'} V_{OO}(R_{O\,j}) \quad (6)$$

The zero of energies was taken for slab at its optimal geometry with oxygen atom at infinite separation.

We have calculated new DFT curves over different sites over the unit cell (Fig. 1(b)). Fig. 2(a) shows these DFT curves as function of Z_O, showing a quite corrugate behavior of the PES. Only the deepest well corresponds to a true minimum in 3D. These new DFT data have been used to check the quality of the new interpolated PES (called hereafter as PES-CRP). Fig. 2(b) proves that PES-CRP curves compare very well with new DFT ones, whose points were not included into the interpolation (excepting for T1 and S2 sites). The errors don't exceed 0.1 eV for Z_O points inside the interval $0 < Z_O < 3$ Å and this PES improves much more the earlier PES-2B [13]. The PES-2B was based only on T1 and S2 DFT data, assuming that the $V^{O\text{-slab}}$ potential (6) was described simply by the two-body terms (i.e., I^{3D} term was neglected).

We give in Fig. 3 contour plots of both PESs for two fixed Z_O values over the unit cell. The presence of T1 minimum can be clearly seen in Fig. 3(b) and 3(d). It is located at $R_{OSi} = 1.560$

Å and θ = 6.3° over a Si atom, with harmonic vibrational frequencies of 833.9, 331.8, and 171.6 cm^{-1}; the T1 minimum adsorption energy is 5.0 eV. These values are similar to those obtained from DFT calculations or from PES-2B, although the minimum energy for PES-CRP is slightly larger due to the slab contribution (V^{slab} = 0.16 and $V^{O\text{-}slab}$ =-5.16 eV). An extensive analysis of PES-CRP shows as well the existence of the more stable T1' minimum (along the diagonal of the unit cell with positive slope), as can be seen in Fig. 3(c), which is not present in PES-2B (Fig. 3(a)). For this minimum (E_{ad} = 7. 10 eV as V^{slab} = 1.68 and $V^{O\text{-}slab}$ = -8.78 eV), the O atom is in between the first and the second layers (i.e., Z_{Oad} = -0.595 Å) at R_{OSi} = 1.551 Å and θ = 112.6°, with a significant reconstruction of the cell (R_{SiSi} = 4.532-4.551 Å) due to a shift of the Si atom away from its equilibrium position (i.e., ΔX_{Si} = -0.181 Å, ΔY_{Si} = -0.618 Å). Its harmonic vibrational frequencies (1197.7, 581.0, 262.3 cm^{-1}) confirm that it is a true minimum. The differences observed between the properties of the T1' minimum in calculations based on DFT and PES-CRP can be explained by the fact that the PES-CRP is based on DFT calculations over a rigid slab at equilibrium geometry and in the use of an empirical slab potential. Nevertheless, PES-CRP gives a quite reasonable description of this minimum as far the dynamical study of this work is concerned. Clearly, studies of internal diffusion would require a better fit of T1' properties and a search of another minima for O inside the slab. In fact, previous theoretical studies of atomic or molecular oxygen with SiO_2 [30-31] or SiO_2/Si [32-33] systems show a clear trend to incorporate these species into the oxide network. Thus, a peroxy linkage configuration forming Si-O-O-Si bond seems to be the most stable atomic configuration [30, 34-35] in the SiO_2 region while a double Si-O-Si bridge structure is the most stable for oxygen ions (e.g., O^- and O^{2-} [31]).

The PES-CRP has been also fruitfully used in the construction of a new DFT PES for studying the ER reaction of O + O_{ad} over β–cristobalite, based also on the CRP method, and whose dynamics study is in progress.

4. Classical dynamics study

We have carried out a dynamics study of atomic gas oxygen colliding with β-cristobalite (100) surface by means of the classical trajectory method [36]. We have included the motion of all atoms in a 9-layer (100) slab, using a 2x2 square surface unit cell (104 atoms in all) with a cell parameter of 7.348 Å. The slab temperature (T_S = 300 - 1100 K) was controlled by means of a Generalized Langevin equation (GLE) approach [36, 37]. The corresponding random and

friction forces were applied only to the atoms in the bottom Si layer of the slab, which are also forced to oscillate around their bulk equilibrium positions (by using extra "springs") to avoid a global translation of the slab. We checked that the empirical slab vibrated with very small fluctuations around the average slab energy corresponding to the selected temperature ($<E>=3Nk_bT_S$), with a maximum error of 50 K. Generalized friction and fluctuating forces balance, according the fluctuation-dissipation theorem, so that the proper temperature is maintained in the primary zone (i.e., the lattice atoms that can interact directly with colliding O atom).

The incident oxygen is located initially at 4-6 Å from the surface and the aiming point (X_O,Y_O) is determined by a random uniform sampling of the square 1x1 unit cell. Its kinetic energy (E_i) is within the range 0.1 - 1.1 eV. The velocity vector is defined by its angle (θ_i) with respect to the negative Z axis and its projection (ϕ_i) onto the X-Y plane. The angle ϕ_i is determined by an uniform random sampling in the interval (0-360º). Two sets of independent calculations were carried out with θ_i equal to 0º and 45º, respectively.

Hamilton's equations were integrated by using a modified Beeman algorithm with a fixed step of Δt = 0.1 fs. Energy was conserved within 10^{-4}-10^{-5} eV in absence of the GLE bath. Batches of 1000-5000 trajectories were integrated for each initial condition (i.e., E_i, θ_i and T_S), which ensures that statistical errors remain below 1%. Trajectories were integrated up to a maximum time of 5 ps. Some tests at longer times (e.g., 10 ps) were also made to check the convergence of reaction probabilities. Two processes may take place: reflection and sticking. The first process implies that the colliding O atom gets a positive Z velocity component and a similar final Z value as the initial one. The sticking process corresponds to those atoms that are not reflected before 5 ps. Those ending below the surface (i.e., $Z_O < 0$ and $v_{Oz} < 0$) are considered as absorbed and the others as adsorbed. Note that PES-CRP has not been determined below Z_O = -1 Å, so that all atoms reaching the latter distance, at whatever time, are considered as absorbed.

In Fig. 4(a) are plotted the sticking and reflection probabilities versus E_i for a fixed T_S at two incident angles (0º and 45º). The sticking probabilities are much higher (90-98 %) than the reflection ones for all the initial conditions in agreement with the previous PES-2B results [13].

There is a slight increase of the sticking probability with increasing the collision energy opposite to PES-2B results. This behavior is also at variance to the typical prediction of simple models of gas-surface collisions (like the hard-cube model (HCM) [38] or the improved Baule model [39]). For instance, HCM assumes that an atom or molecule collides in an attractive

potential with well depth E_{ad} on a solid surface modeled by a cube of effective mass (M_c), which is moving at a velocity from a Maxwell distribution at T_S. In Fig. 4(b), we compare the sticking probability obtained from our trajectory calculations with the HCM predictions at T_S = 500 K, using the adsorption energy for the T1 minimum (i.e., 5.0 eV) and an optimal M_c of 191 amu. The difference is due to the attractive character of PES-CRP, which favors the penetration (i.e., absorption) over the adsorption for both incident angles. Indeed, as can be seen in Fig. 4(b), the absorption probability (P_{ab}) is close to the total sticking probability (P_s), the adsorption probability (P_{ad}) remaining almost constant and below 0.1 for all kinetic energies. The contrary dependence of P_{ad} and P_{ab} with E_i was also observed for PES-2B. However, P_s for PES-2B showed a converse trend with E_i because this PES was much more repulsive, therefore reducing a lot the absorption ($P_{ab} < 0.2$ for $0.1 \leq E_i \leq 1.1$ eV) compared with the adsorption, hence that P_s practically reproduce P_{ad} for PES-2B instead of P_{ab} as in PES-CRP.

Sticking probability corresponds to a total energy scaling, explaining the observed small dependence with the two incident angles, as could be expected due to the high corrugation of the PES-CRP (Fig. 2(b)). This also could explain the differences between the PES-CRP dynamics and the HCM predictions, because this model assumes a flat and structureless surface (i.e., normal energy scaling).

Fig. 5(a) shows that there is a small decrease of the sticking probabilities and consequently an increase of the reflection probabilities with increasing T_S at two fixed collision energies (0.1 and 1 eV) for both incident angles. This is the usual trend observed in PES-2B, also in agreement with HCM prediction (Fig. 5(b)) as higher surface temperatures improve the desorption, diminishing in this way the sticking probabilities. Nevertheless, HCM is not able to reproduce the E_i dependence as was pointed out before. The seemingly similar surface temperature dependence of the sticking probabilities can be explained once again splitting the adsorption and absorption contributions (Fig. 5(b)). Both PESs show that adsorption decreases and absorption increases with T_S augments. The rise of the surface temperature causes that slab atoms can vibrate with larger amplitudes and help thus the penetration or absorption of oxygen atom into the big unit cell of β-cristobalite, in agreement with the results obtained. Previous DFT studies have demonstrated that diffusion of atomic oxygen is quite easy even with smaller units cells of silica (e.g., α-quartz [30-31]). However, in spite of the minor contribution of the adsorption respect to the absorption to the total sticking, the faster decrease of P_{ad} respect to the slower augment of P_{ab} produces that the total sticking decreases with T_S increment.

Similar results have been obtained for other initial conditions (e.g., T_S = 500 K or 700 K and E_i = 0.3 eV or 0.7 eV).

We define the average total oxygen energy for every batch of trajectories that end with sticking by averaging the oxygen kinetic energy (T_O) plus its potential energy ($V^{O\text{-}slab}$) for these trajectories at a given collision time (t_{col}). The latter quantity is plotted in Fig. 6(a) as a function of t_{col} for those trajectories that end in sticking (mostly absorption), for T_S = 700 K, E_i = 0.1 and 1 eV, and θ_i = 0º. It is clearly observed that there is a very quick release (t_{col} < 0.5 ps) of the O kinetic energy to the surface phonons, which enhances O sticking through penetration into the slab. The faster energy exchange at E_i = 1 eV compared with E_i = 0.1 eV is consistent with the larger sticking obtained at higher collision energies (Fig. 4(b) or 5(b)). This means that sticking is a direct process, being the dynamic trapping (indirect process) contribution negligible for this system. This behavior is similar in both absorption and adsorption processes.

The study of the scattering of atomic nitrogen on tungsten (100) [22] showed that the absorption probability (adsorption was prevented due to the frozen surface approximation) was large and decreased with increasing collision energy. The decomposition into direct ($P_{ab(d)}$; trajectories with less than 5 rebounds) and trapping ($P_{ab(t)}$) contributions showed that $P_{ab(d)}$ increases slowly with energy while $P_{ab(t)}$ contribution decreases strongly giving place to the final decrease of total P_{ab} though $P_{ab(d)} > P_{ab(t)}$ (excepting at the lowest E_i). This is in agreement with the P_{ab} behavior of our system, which corresponds mainly to direct absorption, with a slow increase in front of E_i.

Fig. 6(b) and 6(c) show the average final Z coordinate and the average parallel displacement with respect to the initial aiming point over the unit cell of the O atoms that become stuck as a function of collision time in the same conditions as in Fig. 6(a). Z_O achieves quickly values lower than 1 Å, decreasing even more as could be expected due to the geometry of the T1' minimum, which enhances the absorption. The parallel displacement (Fig. 6(c)) is always lower than half the minimum distance between two neighbor Si atoms (i.e., R_{SiSi} = 5.196 Å/2 for a clean slab); therefore, the colliding O atoms (i.e., not reflected) become quickly stuck (direct process) close to the Si atoms along the positive slope diagonal of the unit cell, as can be seen in Fig. 7 for both absorption and adsorption. The absence of O atoms in the second layer along this diagonal (contrary to what happens for the other diagonal) favors the penetration of O inside the slab in agreement with the attractive character of PES-CRP in these T1' sites (Fig. 3(a)). In spite of there is a transition state between T1 and T1' with an energy barrier of 0.78 eV respect T1 (R_{OSi} = 1.556 Å, θ = 49.8°, R_{SiSi} = 4.676 Å, ν_i = 329.9i, 481.3, 247.1 cm^{-1}), the exothermic process for the initial O gas atomic collisions at all E_i values justifies this

predominant absorption. Furthermore, the big size of the unit cell of β-cristobalite, where Si atoms are quite far each other can help more these processes. Moreover, as can be seen in Fig. 7 (b), T1 minimum seem to be determinant to produce the few adsorption trajectories.

A similar result was found in the study of the sticking of atomic oxygen on the Cu (100) surface [21], where the O atoms traveled along the surface less than twice the nearest neighbor distance and therefore there was also an efficient energy dissipation to the surface. Nonetheless, this system presented low reflection and absorption probabilities (<0.005), being adsorption the dominant process, as may be expected by the large adsorption energies (7.1-8.5 eV) at the minimum with Z_O = 0.85 Å, the small lattice constant of 3.633 Å (i.e., minimum Cu-Cu distance of 2.569 Å) and possibly by the metallic nature of the surface. In the case of the sticking of nitrogen on the W(100) surface [22] there is also a small lattice parameter of 3.175 Å, but now the minimum W-W distance is larger (i.e., 3.175 Å) and the existence of a large adsorption energy (7.4 eV) at the centered hollow site (Z_N = 0.63 Å) is counteracted by the also attractive character of the PES in another four sites over the unit cell, which favors the final penetration of the N.

In PES-2B we observed as well a similar behavior with respect the quick energy dissipation and the short parallel motion around the surface, but then the adsorption trajectories were concentrated in a similar extension around all Si atoms of the first layer, while the scarce absorption trajectories preferred too the positive slope diagonal as in PES-CRP, because the absence of O atoms under it.

In order to compare with the limited experimental data on this system, we have calculated thermal initial sticking probabilities (also called initial sticking coefficient (S_o) in some works), sampling the initial conditions of the trajectories from a Boltzmann distribution corresponding to $T_O = T_S$, fixing θ_i to 0º. Fig. 8 shows that S_o decreases with temperature increase as occurred also for PES-2B [13]. We have plotted as well the results for S_o derived from kinetic models for oxygen recombination on reaction-cured glass (RCG) and pure silica [5], although these models assumed an adsorption energy of ~3.5 eV, regardless of the kind of silica surface. Assuming a given value of the adsorption energy (E_{ad}) and the form of S_o as

$$S_o(T) = B \cdot e^{-C \cdot T} \qquad (7)$$

the coefficients (B and C) were optimized to fit oxygen recombination coefficient (γ_O) in these studies [4-5]. The use in these kinetic models of a value of E_{ad} smaller than that corresponding

to PES-CRP should produce lower S_o values, as simple HCM predictions confirm, explaining part of the differences shown in Fig. 8. An alternative model of catalytic reactions on silica surfaces has been proposed by using an expression of the initial sticking coefficient partially based on standard transition state theory approximations, assuming an E_{ad} of 2.60 eV [7]. We have checked [10] that this expression, which depends on the parallel frequencies of the adsorption minimum, provides very low S_o values (e.g., < 0.03 within 300-1900 K) even using the same DFT data as in PES-CRP, increasing also with T in disagreement with HCM and trajectory results. Thus, we believe that trajectory calculations are much more reliable than these simple models in order to compute S_o. Classical trajectories with PES-CRP give much higher initial sticking coefficients as could be expected for the large adsorption energies of T1 and T1' minima, with a reasonable decreasing of S_o with T augment. It is therefore clear that the derivation of "empirical" $\gamma_O(T)$ or $\gamma_N(T)$ require reliable models for oxygen or nitrogen atomic sticking.

Finally, the solid structure (i.e., β-cristobalite, β-quartz, amorphous silica,…) can affect also these initial sticking coefficients, as shown for the oxygen recombination coefficient over β-quartz compared with β-cristobalite [8-9], explaining part of the differences in Fig. 8.

5. Concluding remarks

The main goal of this work has been to investigate the interaction of atomic oxygen with the β-cristobalite (100) surface by means of DFT and classical trajectory method. The construction of a full dimensional PES based on extensive DFT data and some empirical potentials of silica allows understanding the dynamics of this system. The existence of two adsorption minima (T1 and T1') involving a silicon atom of the first layer, with large adsorption energies and a low energy barrier between them, seem to play a key role in the dynamics of the sticking processes.

The sticking probabilities are much more higher (>0.9) than the reflection ones for all initial conditions (T_S = 300-1100 K, E_i = 0.1 - 1eV, θ_i = 0º, 45º). They increase with collision energy and decrease with surface temperature. The analysis of the sticking processes shows that there are two types of trajectories (adsorption and absorption/penetration) with different behavior. The attractive character of PES-CRP at short O-surface distances (mainly at T1' minima) favors absorption at the expense of adsorption for both incident angles. This trend is consistent with earlier theoretical studies of atomic or molecular oxygen with SiO_2 or SiO_2/Si systems [31, 34,

35], which established the capacity of silicon oxide to incorporate these species by forming peroxy Si-O-O-Si linkages or double Si-O-Si bridges.

Previous PES-2B, derived with few DFT data, showed large sticking probabilities too, but the main process was adsorption due to the more repulsive character of the latter PES under O penetration into the slab. Thus, PES-CRP seems to be much more accurate as it includes a dense grid DFT data and agrees also with previous DFT results for O/SiO_2 or O_2/SiO_2 systems.

Sticking probability corresponds to a total energy scaling, explaining the observed small dependence with the incident angle and also in agreement with the high corrugation of PES-CRP. The slow increase of the absorption probability (with $P_s \approx P_{ab}$) as a function of E_i can be explained by the direct mechanism (not dynamic trapping) observed in all absorbed trajectories, with a quick dissipation of the oxygen energy into the slab combined with a very short parallel displacement over the unit cell, which facilitates the O penetration into the slab through T1 and T1' PES-CRP minima.

Calculated thermal initial sticking coefficients are much higher than semiempirical values derived for RCG and pure silica, although these apparent discrepancies could be caused by the difference in both the SiO_2 structure and the adsorption energy introduced in the kinetic models. The simple expressions derived in [7] from standard transition state theory predict too low thermal initial sticking coefficients compared with more trustworthy classical dynamics results. Hence some semiempirical kinetic models for oxygen or nitrogen atomic recombination over silica should be revisited.

Finally, the huge fraction of oxygen absorption in β-cristobalite can reduce considerably the extension of the oxygen Eley-Rideal recombination, as could be expected because the incoming O atoms will interact mainly with a few adsorbed atoms.

Acknowledgments

This work has been supported by the Spanish Ministry of Education and Science (Projects ref. CTQ2006-02195 and UNBA05-33-001) and by the Autonomous Government of Catalonia (Projects ref. 2005SGR00175 and 2005 PEIR 0051/69). The authors are grateful to the Computer Centre of Catalonia (CESCA) for providing a part of the computer time.

References

[1] G.S.R. Sarma, in: M. Capitelli (ed.) , Molecular Physics and Hypersonic Flows, NATO ASI Series C, vol. 482 (Kluwer Academic Publishers, Dordrecht, 1996) p. 1

[2] V. L. Kovalev, A. F. Kolesnikov, Fluid. Dyn. 40 (2005) 669.

[3] T. Kurotaki, AIAA paper 2000-2366 (2000).

[4] W. A. Seward, E. J. Jumper, Therm. Heat Trans. 5 (1991) 284.

[5] E. J. Jumper, W. A. Seward, J. Therm. Heat Trans. 8 (1994) 460.

[6] F. Nasuti, M. Barbato, C. Bruno, J. Therm. Heat Trans. 10 (1996) 131.

[7] A. Daiss, H.-H. Frühauf, E. W. Messerschmid, J. Therm. Heat Trans. 11 (1997) 346.

[8] M. J. H. Balat, M. Czerniak, J. M. J. Badie, Space Rock 36 (1999) 273.

[9] M. Balat-Pichelin, J. M. Badie, R. Berjoan, P. Boubert, Chem. Phys. 291 (2003) 181.

[10] C. Arasa, P. Gamallo, R. Sayós, J. Phys. Chem. B 109 (2005) 14954.

[11] R. W. G. Wyckoff, Crystal Structures (Interscience, New York, 1965).

[12] R. B. Sosman, The Phases of Silica (Rutgers Univ. Press, New Brunswick, 1965).

[13] C.Arasa, H. F. Busnengo, A. Salin, R. Sayós, Proceedings of the 25th International Symposium on Rarefied Gas Dynamics, M.S.Ivanov and A.K.Rebrov (ed.) (2007), Chap. 7, p. 666

[14] G. Kresse, J. Hafner, Phys. Rev. B 47(1993) 558.

[15] G. Kresse, J. Hafner, Phys. Rev. B 48 (1993) 13115.

[16] G. Kresse, J. Furthmüller, Comput. Mater. Sci 6 (1996) 15.

[17] G. Kresse, J. Furthmüller, Phys. Rev. B 54 (1996) 11169.

[18] A. F. Wright, A. J. Leadbetter, Philos. Mag. 31 (1975) 1391.

[19] M. O. Keefe, B. G. Hyde, Acta Crystallogr. B32 (1976) 2923.

[20] J. Behler, B. Delley, S. Lorenz, K. Reuter, M. Scheffler , Phys. Rev. Lett. 94 (2005) 036104-1.

[21] N. Perron, N. Pineau, E. Arquis, J. C. Rayez, A. Salin, Surf. Sci. 599 (2005) 160.

[22] G. Volpilhac, H. F. Busnengo, W. Dong, A. Salin, Surf. Sci. 544 (2003) 329.

[23] M. Rutigliano, A. Pieretti, M. Cacciatore, N. Sanna, V. Barone, Surf. Sci. 600 (2006) 4239.

[24] A. B. Rosenthal, S. H. Garofalini, J. Am. Ceram. Soc. 70 (1987) 821.

[25] S. H. Garofalini, J. Chem. Phys. 76 (1982) 3189.

[26] H. F. Busnengo, A. Salin, W. Dong, J. Chem. Phys. 112 (2000) 7641.

[27] P. Rivière, H. F. Busnengo, F. Martin, J. Chem. Phys. 121 (2004) 751.

[28] N. Pineau, H. F. Busnengo, J. C. Rayez, A. Salin, J. Chem. Phys. 122 (2005) 214705.

[29] H. F. Busnengo, M. A. Di Césare, W. Dong, A. Salin, Phys. Rev. B 72 (2005) 125411.

[30] D.R. Hamann, Phys. Rev. Lett. 81 (1998) 3447

[31] Y. Gin, K.J. Chang, Phys. Rev. Lett. 86 (2001) 1793

[32] W. Orellana, A.J.R. da Silva, A. Fazzio, Phys. Rev. Lett. 90 (2003) 16103-1

[33] A. Bongiorno, A. Pasquarello, Phys. Rev. Lett. 93 (2004) 086102-1

[34] T. Akiyama, H. Kageshima, Surf. Sci. 216 (2003) 270

[35] T. Akiyama, H. Kageshima, Surf. Sci. 576 (2005) L65

[36] G.D. Billing, Dynamics of Molecule Surface Interactions (John Wiley & Sons, New York, 2000), chap. 5 and 6.

[37] J. C. Tully, J. Chem. Phys. 73 (1980) 1975

[38] A. Gross, Theoretical Surface Science (Springer Verlag, Berlin, 2003), chap. 6.

[39] R. I. Masel, Principles of Adsorption and Reaction on Solid Surfaces (John Wiley & Sons, New York, 1996), chap. 5.

Figure captions

Fig. 1

Fdd2 β-cristobalite (100) unit cell: a) the triangle shows the irreductible zone used to define the grid of DFT points and b) additional sites used to check the interpolated PES. Numbers indicate the surface layer. Black spheres are Si atoms and white spheres O atoms.

Fig. 2

Potential energy for an O atom over different sites of a frozen β-cristobalite (100) surface as a function of Z_O distance to the surface: a) DFT results. Lines are used to guide the eye. b) interpolated results (PES-CRP) for the sites no used in the definition of the interpolation (excepting for T1 and S2).

Fig. 3

Contour plots of both PESs for an O atom over a frozen β-cristobalite (100) surface. Each panel corresponds to a fixed Z_O value, namely (a) PES-2B, Z_O = -0.5 Å, (b) PES-2B, Z_O = 1.56 Å, (c) PES-CRP, Z_O = -0.5 Å and (d) PES-CRP, Z_O = 1.56 Å. The energy difference between contours is 0.5 eV. Dashed line shows the square unit cell. T1 and T1' minima are shown.

Fig. 4

Sticking and reflection probabilities for an O atom over a β-cristobalite (100) surface: (a) vs. O kinetic energy for T_S=500 K and for two incident angles: 0º (solid line) and 45º (dashed line), and b) comparison of the sticking (circles) and absorption (squares) probabilities for two incident angles with the HCM prediction (dotted line).

Fig. 5

Sticking and reflection probabilities for an O atom over a β-cristobalite (100) surface: (a) vs. surface temperature for two incident angles: 0º (solid line) and 45º (dashed line) and two

collision energies: 0.1 (squares) and 1 eV (circles), and (b): comparison of the sticking (solid line) and absorption (dashed line) probabilities for $\theta_i = 0^o$ with the HCM predictions (dotted line) at both collision energies.

Fig. 6

(a) Average total oxygen energy, (b) average final Z_O coordinate and (c) average parallel displacement of O as a function of time for trajectories ending in O sticking, with $T_S = 700$ K, $E_i = 0.1$ (dotted line) and 1 eV (solid line) and $\theta_i = 0^o$.

Fig. 7

Final oxygen positions (X_O,Y_O) corresponding to: a) absorption processes and b) adsorption processes, for a total batch of trajectories (~ 7800) with $T_S = 700$ K, $E_i = 0.1$ eV and $\theta_i = 0^o$. Big circles show Si atoms of the first layer.

Fig. 8

Comparison of calculated thermal initial sticking coefficients of atomic oxygen over β-cristobalite (100) with indirect experimental data derived for RCG and silica [5].

Figure 1

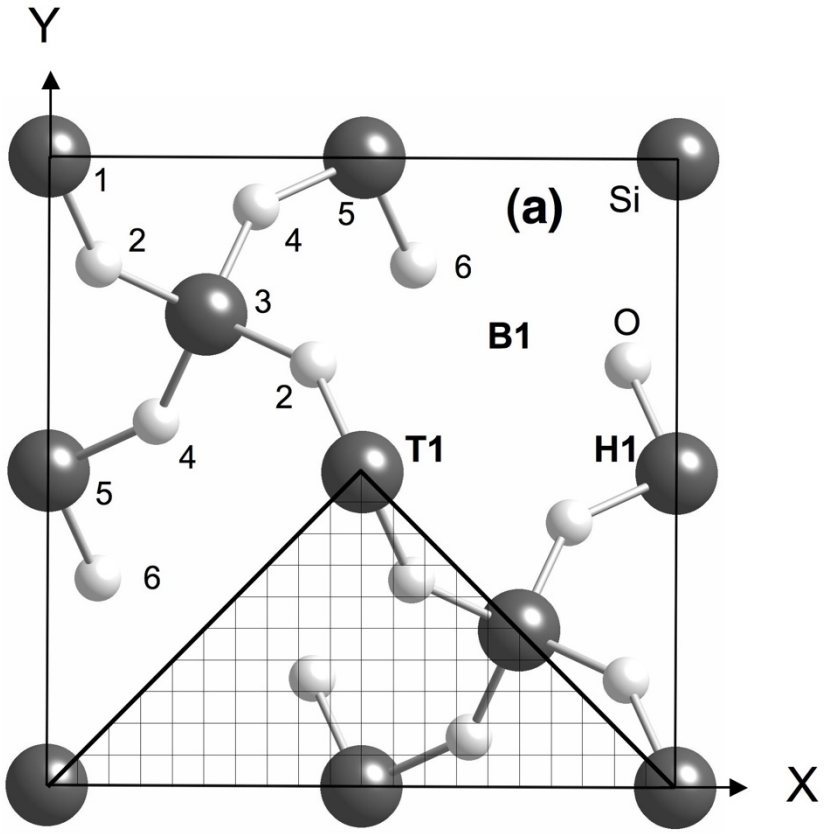
Y
(a)
Si
O
B1
T1
H1
1
2
3
4
5
6
X

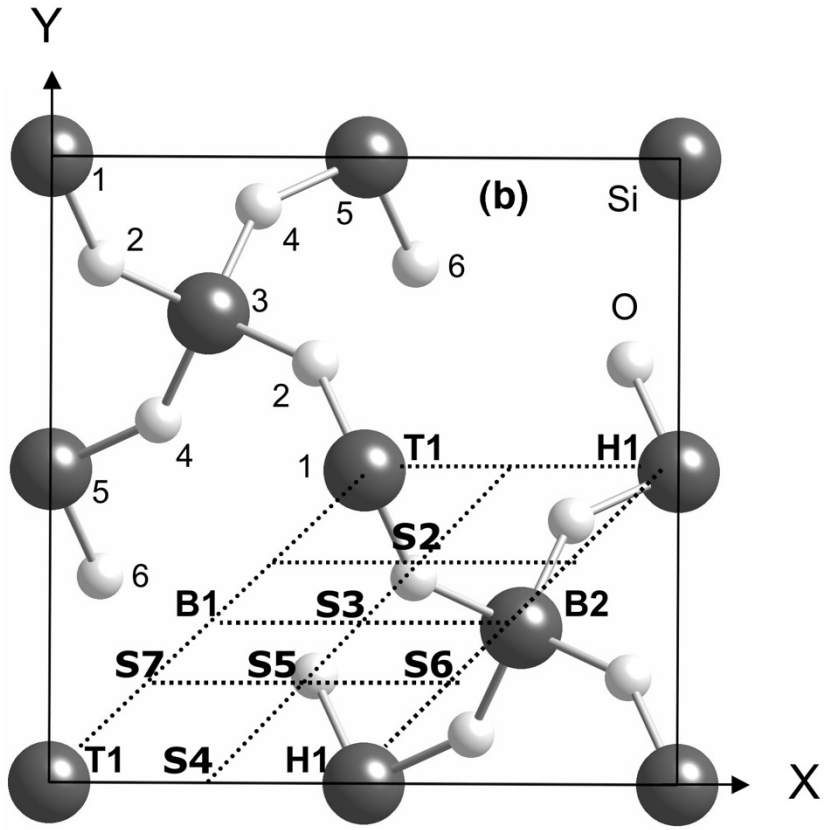
Y
(b)
Si
O
T1
H1
B1
B2
S2
S3
S4
S5
S6
S7
1
2
3
4
5
6
X

Figure 2

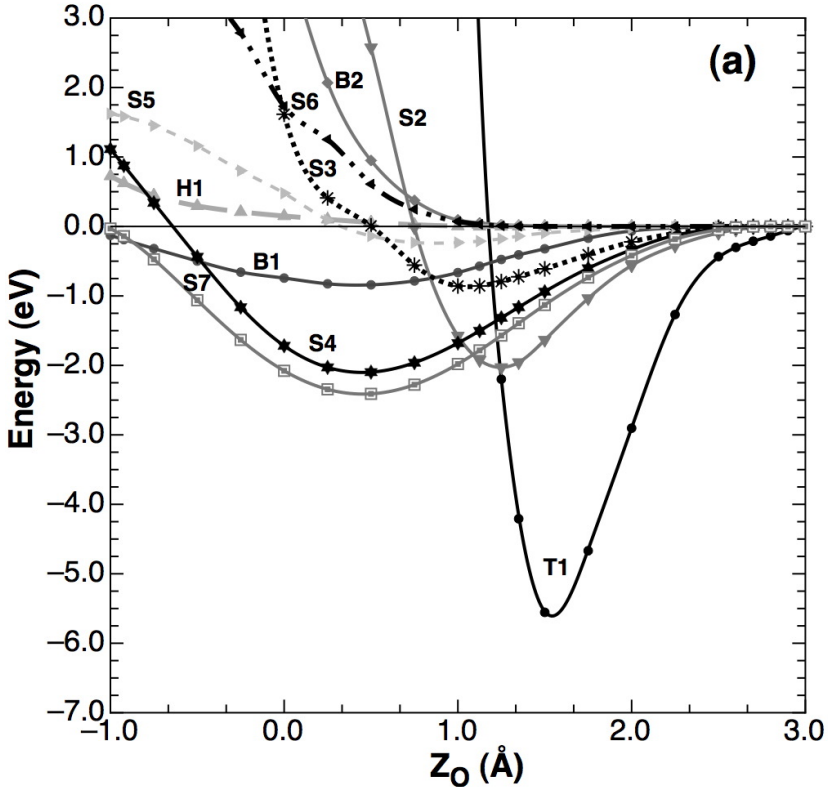
(a)
S5
S6
B2
S2
S3
H1
B1
S7
S4
T1
Energy (eV)
Z_O (Å)

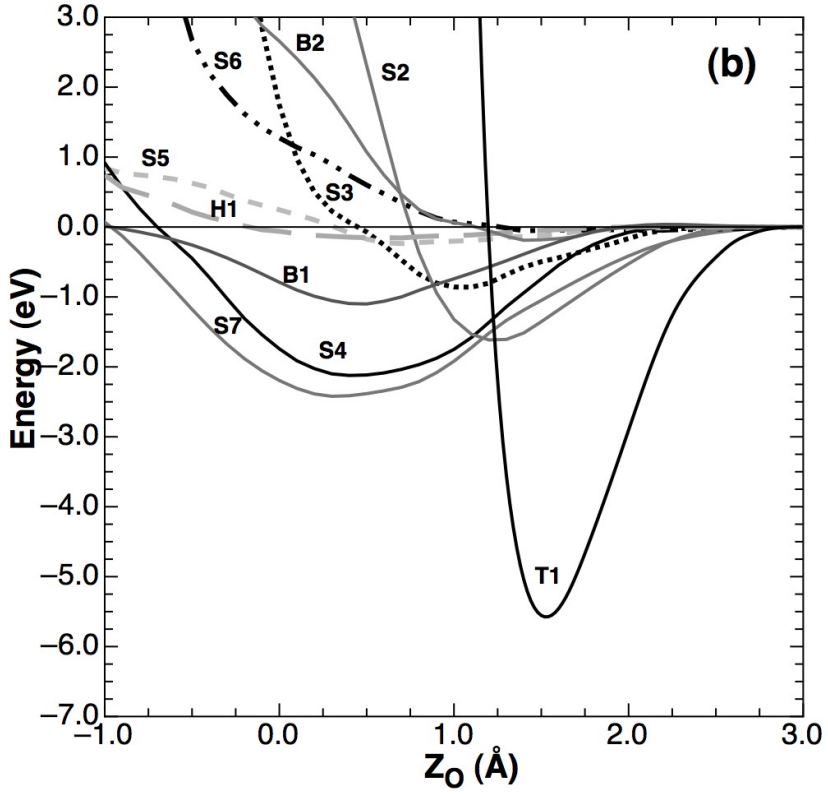
(b)
S6
B2
S2
S5
S3
H1
B1
S7
S4
T1
Energy (eV)
Z_O (Å)

Figure 3

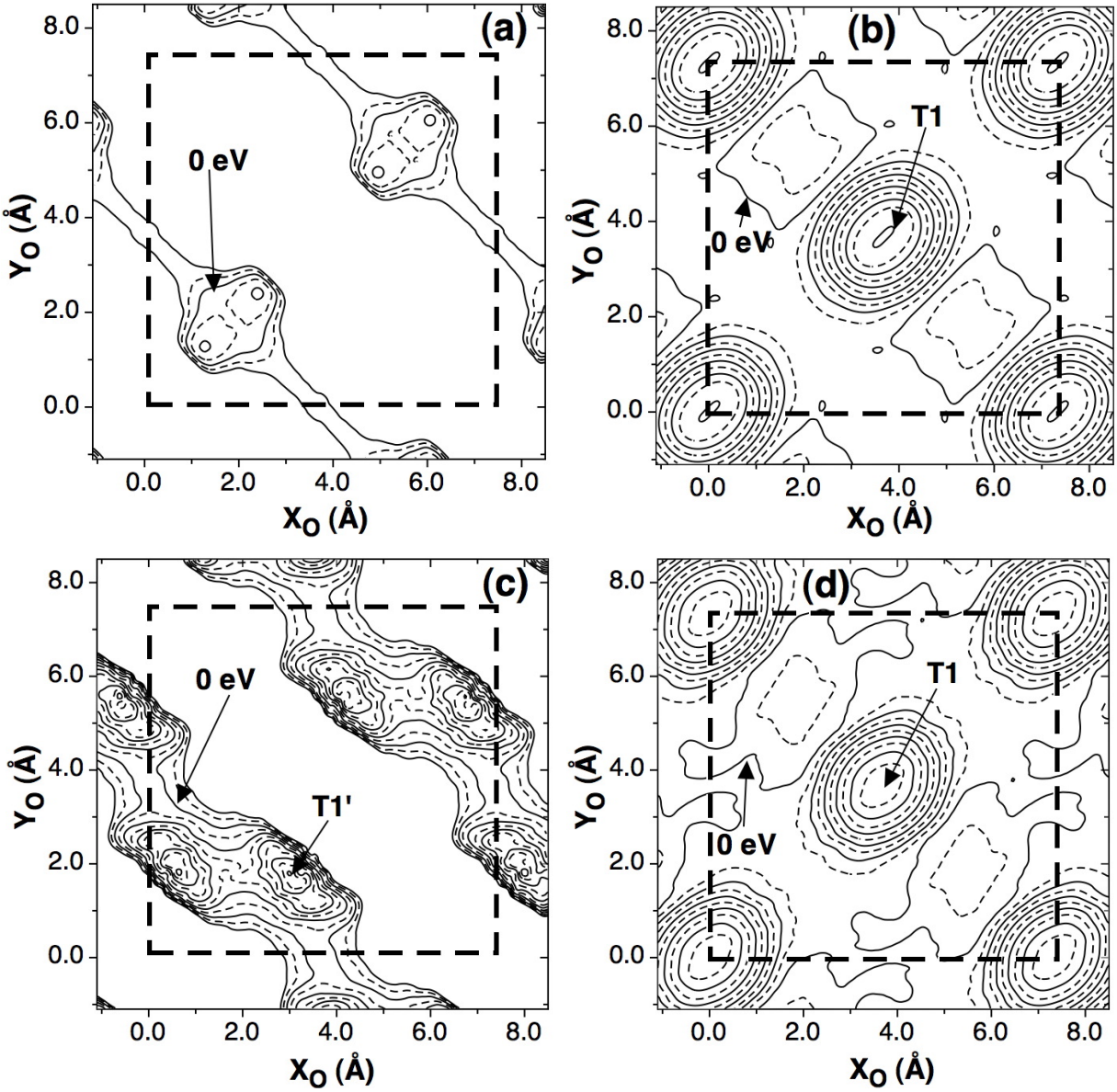

Figure 4

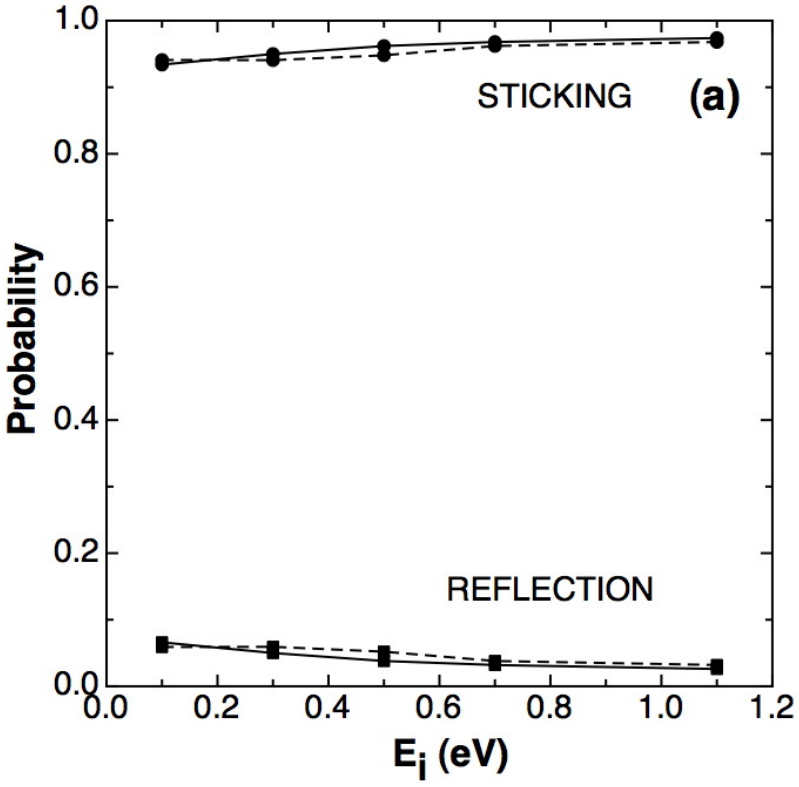
1.0
0.8
0.6
0.4
0.2
0.0
Probability
STICKING
(a)
REFLECTION
0.0
0.2
0.4
0.6
0.8
1.0
1.2
E_i (eV)

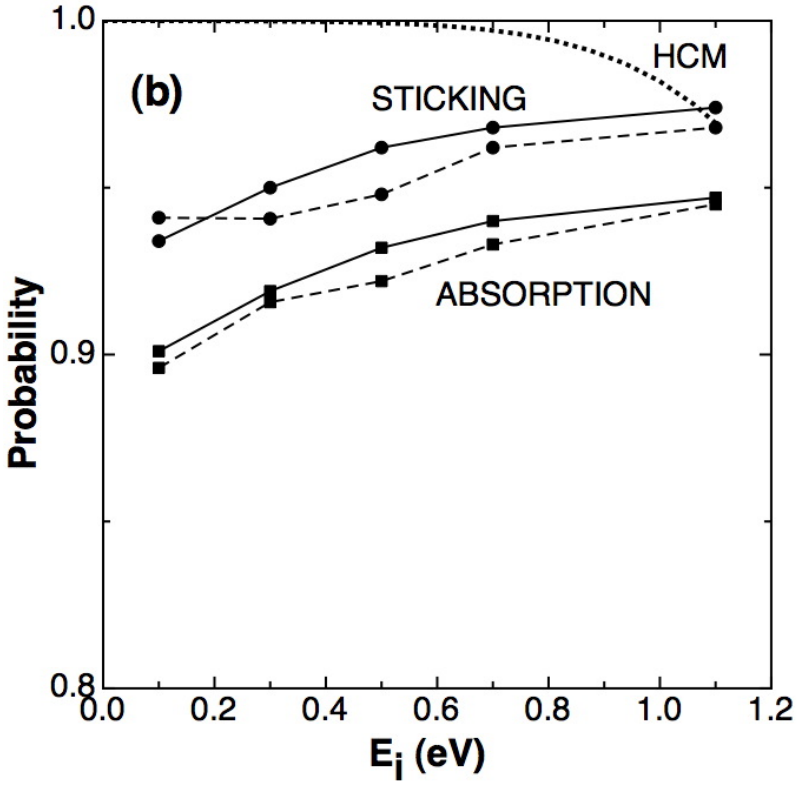
1.0
0.9
0.8
Probability
(b)
HCM
STICKING
ABSORPTION
0.0
0.2
0.4
0.6
0.8
1.0
1.2
E_i (eV)

Figure 5

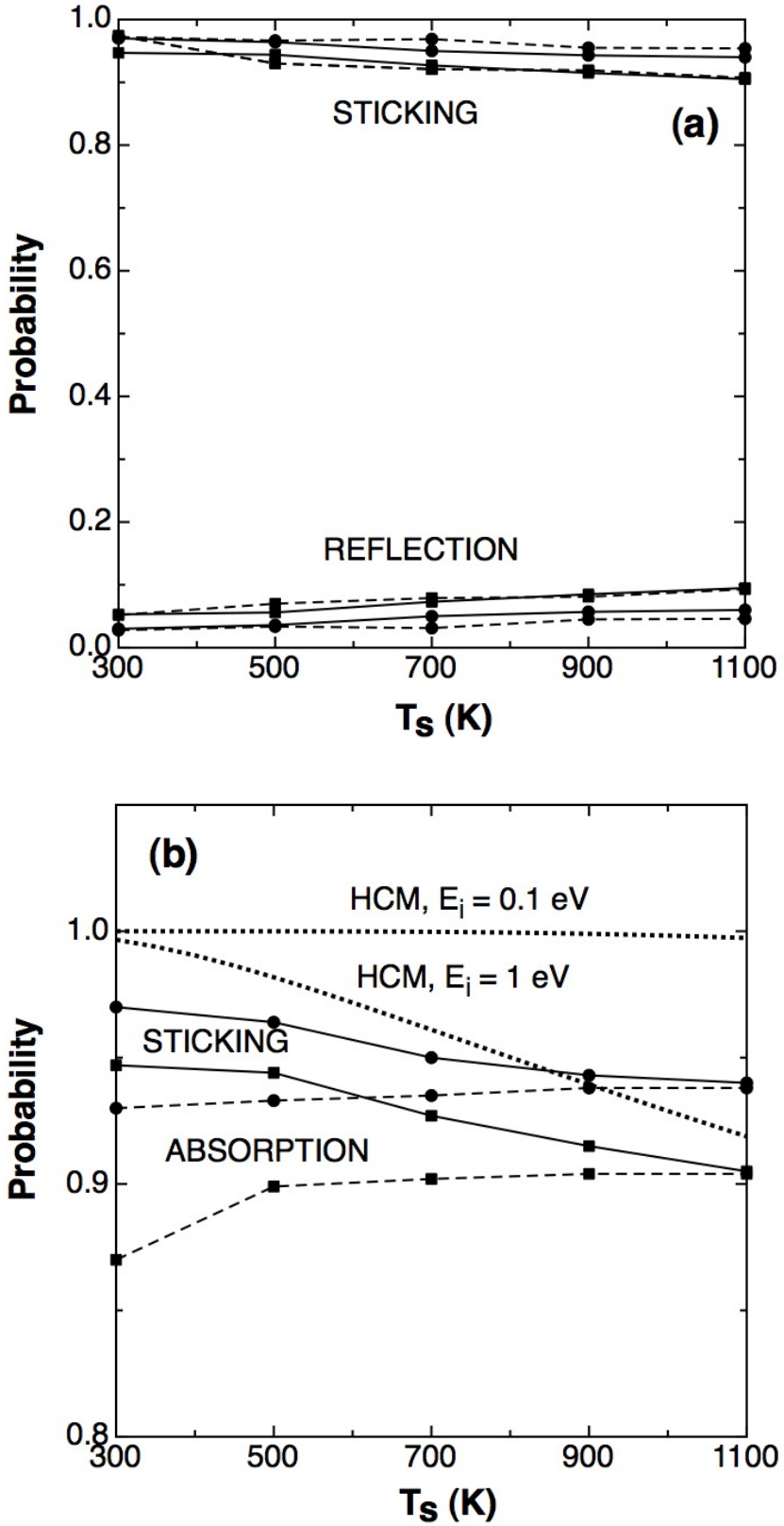
(a)
STICKING
REFLECTION
Probability
1.0
0.8
0.6
0.4
0.2
0.0
300
500
700
900
1100
Ts (K)
(b)
HCM, Ei = 0.1 eV
HCM, Ei = 1 eV
STICKING
ABSORPTION
Probability
1.0
0.9
0.8
300
500
700
900
1100
Ts (K)

Figure 6

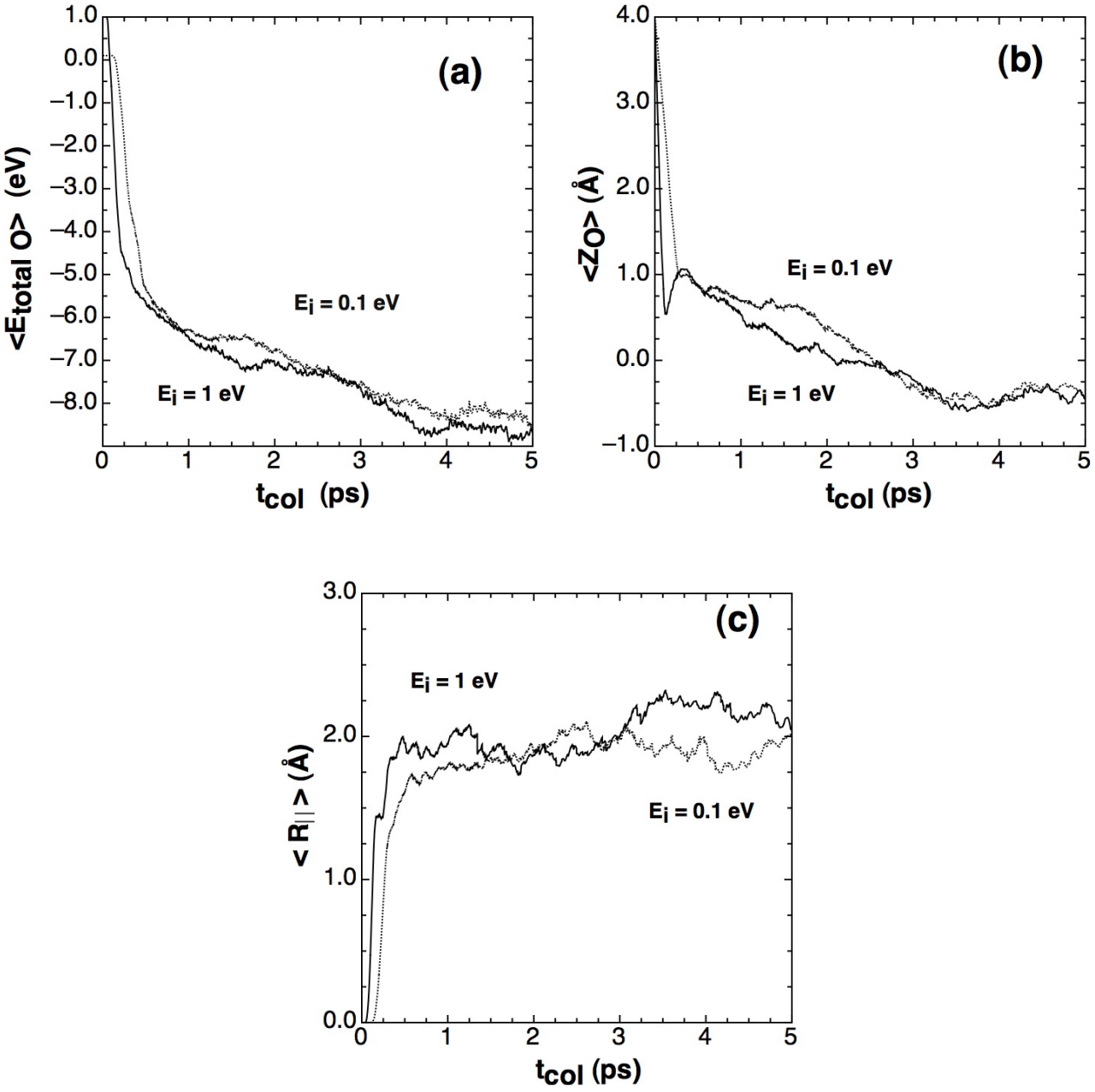
(a)
<E_total O> (eV)
E_i = 0.1 eV
E_i = 1 eV
t_col (ps)
(b)
<Z_O> (Å)
E_i = 0.1 eV
E_i = 1 eV
t_col (ps)
(c)
E_i = 1 eV
E_i = 0.1 eV
< R_|| > (Å)
t_col (ps)

Figure 7

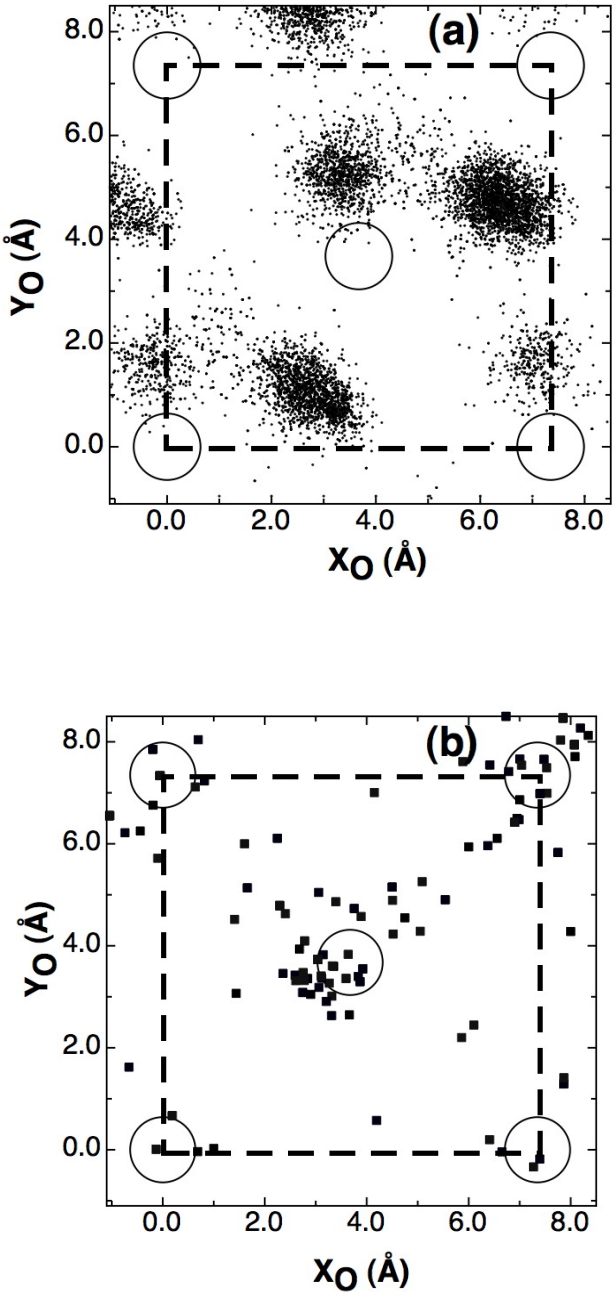

Figure 8

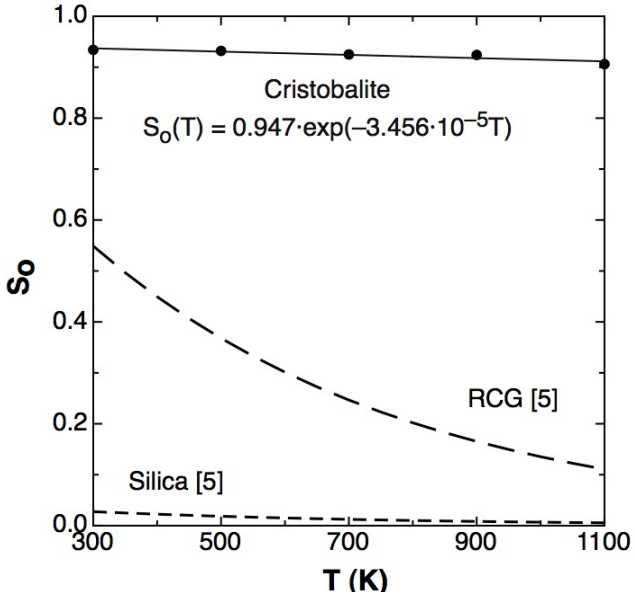
1.0
0.8
0.6
0.4
0.2
0.0
So
Cristobalite
So(T) = 0.947·exp(–3.456·10–5T)
RCG [5]
Silica [5]
300
500
700
900
1100
T (K)